J Nanopart Res (2023) 25:74
https://doi.org/10.1007/s11051-023-05697-3

RESEARCH PAPER

Effect of halloysite nanotubes (HNTs) and organic montmorillonite (OMMT) on the performance and mechanism of flame retardant-modified asphalt

Yangwei Tan · Jianguang Xie · Zhanqi Wang · Kuan Li · Zhaoyi He

Received: 11 December 2022 / Accepted: 23 February 2023 / Published online: 1 April 2023

Abstract Nano-clays and flame retardant composite-modified asphalt has obvious synergistic effects, but the effect of nano-clays on the flame retardant properties, rheological properties, and flame retardant mechanism of flame retardant-modified asphalt has not been studied. In this paper, synergistic flame retardants containing nano-clays and targeted flame retardant (TFR) were prepared and used as nanocomposite flame retardant (NCFR) to modified asphalt (NFRMA). Nano-clays are two types of nano-silicate clays: halloysite nanotubes (HNTs) and organic nano-montmorillonite (OMMT). The flame retardant properties, rheological properties, and flame retardant mechanism of NFRMA have been studied. The results show that the two kinds of NFRMA exhibit obvious synergistic effects. Among them, HNTs can significantly increase the limiting oxygen index and self-ignition temperature of flame retardant asphalt, but OMMT can significantly inhibit the generation of smoke in asphalt combustion process. Both HNTs and OMMT can effectively improve the high-temperature performance of asphalt. The effect of HNTs in improving the high-temperature performance of asphalt is more obvious than that of OMMT. At the same time, HNTs can also improve the degradation of low-temperature performance of asphalt by TFR. However, OMMT will further deteriorate the low-temperature performance of asphalt. The flame retardant enhancement mechanism of HNTs and OMMT mainly enhances the flame retardant performance of asphalt through its own decomposition and heat absorption and improvement of the barrier layer structure. HNTs are more efficient in improving the integrity of the barrier layer, while OMMT exhibits better smoke suppression performance.

Keywords Asphalt · Nano-clays · Nano-architectonics · Flame retardant performance · Rheological properties · Flame retardant mechanism

Highlights
- Synergistic enhancement effect of HNTs and OMMT combined with TFR on flame retardancy of asphalt was found.
- The effect of HNTs and OMMT on the rheological properties of asphalt modified by TFR was studied.
- The synergistic enhancement mechanism of HNTs and OMMT on flame retardant performance of asphalt was discussed based on TGA-DSC, TG-FTIR, and DIP-SEM.

This article is part of the topical collection: "*Part of S.I Nanoarchitectonics for Functional Particles and Materials*"

Y. Tan · J. Xie (✉) · Z. Wang · K. Li
Department of Civil and Airport Engineering, Nanjing University of Aeronautics and Astronautics, 29 Jiangjun Road, Nanjing 211106, Jiangsu, China
e-mail: xiejg@nuaa.edu.cn

Y. Tan
e-mail: tanyw07@nuaa.edu.cn

Z. He
Department of Civil Engineering, Chongqing Jiaotong University, Chongqing 400074, China

Introduction

Asphalt pavement has become the mainstream of tunnel pavement because of its advantages of comfortable

driving, good skid resistance, and easy maintenance [1, 2]. However, asphalt as a polymer material is easily ignited, so how to improve the fire safety of asphalt pavement has become a key topic of tunnel construction and operation [3, 4]. The most effective and common way to improve the flame retardancy of asphalt is to add flame retardant directly to asphalt [5].

At present, the main types of flame retardants are inorganic metal hydroxides [6–8], phosphorus flame retardants [9], and halogen flame retardants [10]. However, due to the low flame retardant efficiency when inorganic metal hydroxides and organic phosphorus flame retardants are used alone [11, 12], the combination of organic and inorganic flame retardants is an important means to improve the flame retardant efficiency [13, 14]. Halogenated flame retardants with high-flame retardant efficiency have been limited to use because it will release toxic gases at high temperatures which can endanger the safety of construction personnel and also hinder escape and fire rescue in a fire. Fu et al. [15] proposed the use of nontoxic halogenated flame retardant derivatives to improve the fire safety of asphalt. The flame retardants used above still have shortcomings such as low flame retardant efficiency, poor economic benefits, and deterioration of mechanical properties of asphalt [1, 5].

With the wide application of nanotechnology in road engineering [15, 16], and extensive research on nanocomposite flame retardants in polymer materials [17–19]; researchers began to use nano-clays to enhance the flame retardant properties of asphalt such as MMT [20, 21] and layered metal hydroxides (LDHs) [22–24]. Zhang et al. [21] found that the main reason for nano-layered silicate to improve the flame retardant performance of asphalt was that it played the role of barrier layer. Zhu et al. [23] and Shen et al.[25] found that LDHs not only have an endothermic and flame retardant mechanism similar to inorganic metal hydroxides, but also exhibit a barrier layer mechanism of nano-layered materials, so it can be used as flame retardants to improve the flame retardant performance of asphalt. However, it may be due to the poor dispersion of nano-clays in asphalt; the addition of nano-clays alone to improve the flame retardant performances of asphalt are not obvious [22, 25, 26], so researchers started to improve the flame retardant performances of asphalt by compounding nano-clays and conventional flame retardants. Bonati et al. [27] found that asphalt modified by nano-clays and aluminum hydroxide (ATH) has obvious synergistic effect, which can significantly enhance the flame retardant properties and effectively improve the physical properties of asphalt. Liang et al. [28] studied the effect of layered silicate compound metal hydroxide on the flame retardant properties of asphalt. It was found that layered nano-silicate was exfoliated in asphalt and showed gas–solid composite flame retardant mechanism. Yang et al. [29] found that OMMT/ATH composite flame retardant-modified asphalt can not only significantly improve the flame retardant performances of asphalt, but also effectively inhibit the production of organic volatiles in the asphalt mixing process. Furthermore, in our previous researches, it was found that the use of tubular silicate clay (halloysite nanotubes (HNTs)) compound flame retardant-modified asphalt can effectively improve the flame retardant efficiency and significantly improve the road performance of asphalt [30–32]. The above nano-clays have synergistic enhancement effects on flame retardants in modified asphalt. At present, there is a lack of research on the effect of nano-clays on the performance and mechanism of flame retardant-modified asphalt.

In this paper, targeted flame retardant asphalt system with organic–inorganic composite flame retardant is firstly prepared, and two kinds of nano-clays (OMMT and HNTs) are added to prepare nano-clays composite flame retardant-modified asphalt (NFRMA). Then, the effects of two kinds of nano-clays on static and dynamic flame retardant properties, high- and low-temperature rheological properties, and flame retardant mechanism of asphalt modified by targeted flame retardant were studied. Furthermore, based on thermogravimetric analysis of flame retardant asphalt, the change of gaseous products, and macro- and micromorphology of the residue, the synergistic enhancement mechanism of two kinds of nano-clays on flame retardant asphalt was explored. The research provides a reference for the subsequent research and application of NFRMA.

Materials and experiments

Materials

Asphalt

The contrast asphalt is styrene–butadiene–styrene block polymer (SBS)-modified asphalt (MA), and its basic physical properties are shown in Table 1.

Table 1 The physical properties of modified asphalt

Type	Penetration (25℃)/(0.1 mm)	Ductility (5℃)/cm	Softening point/℃
Measured value	51.9	33	71.5
Test method	D5-06	D113-07	D36-06

Targeted flame retardant

TFR is a composite flame retardant composed of organic flame retardant diethyl-phosphate aluminum (ADP) and inorganic flame retardant alumina trihydrate (ATH) according to the combustion characteristics of asphalt [30, 31]. The physical and chemical properties of flame retardants are shown in Table 2. Among them, the flame retardant mechanism of ADP mainly produces phosphorus-based free radicals to interrupt the combustion process and produce organic phosphoric acid to catalyze pitch into charcoal, which has gas phase flame retardant and condensed phase flame retardant [33]. The flame retardant mechanism of ATH is that when it is decomposed by heat, it absorbs a lot of heat and produces water vapor and Al_2O_3; it can play the dual role of flame retardant and smoke suppression [34].

Nano-clays

The two kinds of nano-clays used in this paper are HNTs and OMMT. The material composition is shown in Table 3. The geometry structure of HNTs and OMMT is shown in Fig. 1 and Fig. 2. HNTs are tubular nano-silicates [35], which is formed by natural curling of nano-layered silicates. The outer surface of the convoluted laminated silicate is an oxy-silica tetrahedron with good hydrophobicity. The interlayer of silicate sheets is water-binding, which can play a role in heat-absorbing and fire-retardant under high temperature and make the tubular structure of HNTs break up to form smaller sheets. The HNTs were purchased from Yuanxin Nano Technology Co., Ltd., and their particle sizes were in the range of 20–200 nm, with an average particle size of 38.5 nm. OMMT is a multilayer nano-silicate. The two sides of a single-layer sheet are Si–O tetrahedrons, and the middle is a sandwich structure of Al-O octahedrons [36]. $C_{21}H_{46}NCl$ was used to replace the interlayer bound water to increase the interlayer spacing and improve the dispersibility in asphalt. OMMT was purchased from Zhejiang Fenghong New Materials Co., Ltd., and their particle sizes were in the range of 20–200 nm, with an average particle size of 96.3 nm.

Preparation of NFRMA

In order to ensure good dispersion of nano-clays in asphalt, NFRMA was prepared by two-step method [37, 38]. Firstly, asphalt was heated to 160 °C, and nano-clays was added, and the nano-clay-modified asphalt was prepared by shearing at 5000 rpm for 60 min using a high-speed shearing machine, and then TFR was added into asphalt by stirring at 500 rpm for 5 min using a high-speed shearing machine to prepare NFRMA. The composition of NFRMA is shown in Table 4.

Table 2 The physical and chemical properties of flame retardants

Materials	Main composition (%)		Loss (%)	Moisture content (%)	Average particle size	Appearance
ATH	$Al_2O_3 \geq 64.0$	$Fe_2O_3 \leq 0.02$	33.2	0.8	1.6–2.6 μm	White powder
ADP	$P \geq 40.8$	$Al \geq 12.2$	59.5	0.15	10–50 μm	White powder

Table 3 The chemical composition of nano-clays

Chemical composition (%)	SiO_2	Al_2O_3	Fe_2O_3	CaO	MgO	MnO	TiO_2
HNTs	45.8	37.3	0.5	0.25	0.18	0.01	0.01
OMMT	55.0	16.54	0.21	3.97	5.14	0.007	0.02

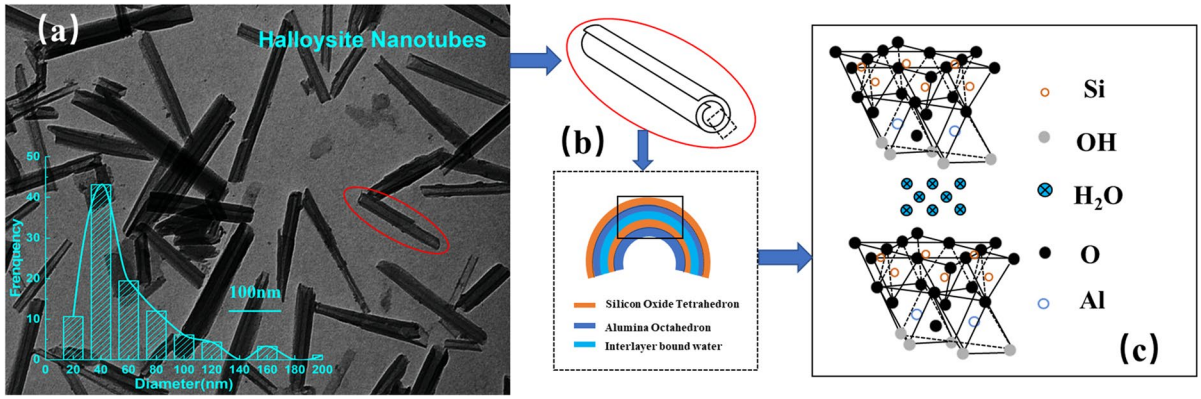

Fig. 1 The geometry structure of HNTs

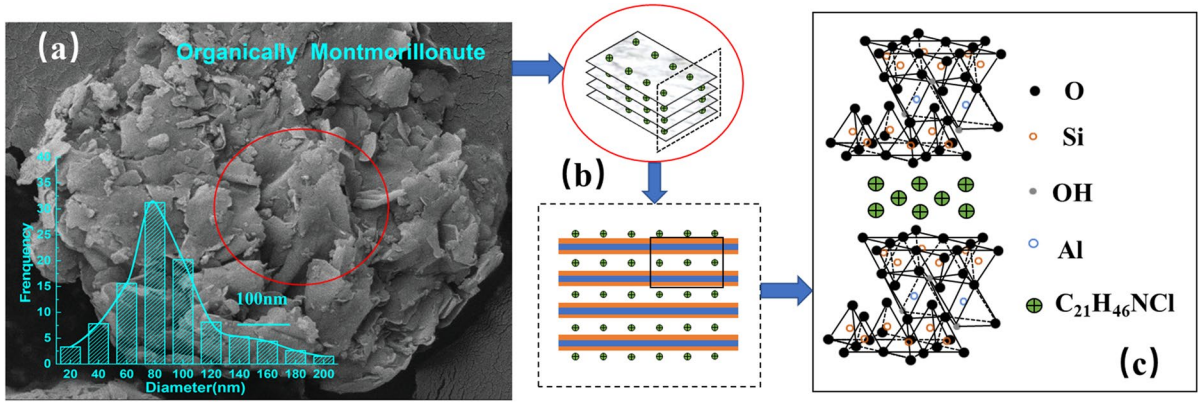

Fig. 2 The geometry structure of OMMT

Characterization and measurements

Flame retardant performance test

Limit oxygen index (LOI) refers to the limit oxygen concentration required to maintain the combustion of asphalt samples, and the equation is shown in Eq. (1). According to ASTM D2863-19, the sample size was 10 cm × 1 cm × 0.5 cm. The JF-3 limit oxygen index instrument of Chongqing Sanzhong Instrument Co., Ltd. was used for testing.

$$LOI = \frac{[O_2]}{[N_2] + [O_2]} \times 100\% \quad (1)$$

In Eq. (1), $[O_2]$ is volume flow of oxygen under critical condition, and $[N_2]$ is volume flow rate of nitrogen under critical conditions.

The self-ignition temperature refers to the temperature at which the asphalt begins to burn after heating [39]. According to AASHTO T48, the Cleveland Opening Cup of Shanghai Precision Instrument Co., Ltd. was used for testing.

The cone calorimeter is a small fire simulator, which truly reflects the combustion characteristics of materials under thermal radiation, such as heat release rate (HRR), smoke produce rate (SPR), total heat release (THR), and total smoke release (TSR). The data obtained by cone calorimeter test (CCT) have good correlation with the real fire situation, which are commonly used to characterize the dynamic combustion properties of asphalt. In this paper, the dynamic combustion properties of asphalt were tested by cone

Table 4 The composition of NFRMA

Type		Asphalt	TFR	HNTs	OMMT
MA		100	-	-	-
MA/TFR		100	8	-	-
MA/HNTs		100	-	1.0	
MA/OMMT		100	-	-	3.0
MA/TFR/HNTs	MA/TFR/0.5%HNTs	100	8	0.5	-
	MA/TFR/1.0%HNTs	100	8	1.0	-
	MA/TFR/1.5%HNTs	100	8	1.5	-
	MA/TFR/2.0%HNTs	100	8	2.0	-
MA/TFR/OMMT	MA/TFR/1.0%OMMT	100	8	-	1.0
	MA/TFR/3.0%OMMT	100	8	-	2.0
	MA/TFR/3.0%OMMT	100	8	-	3.0
	MA/TFR/4.0%OMMT	100	8	-	4.0

calorimeter produced by Fire Testing Technology, London, UK, under the thermal radiation intensity of 50kw/m^2 and air atmosphere [40, 41].

Rheological performance test

The high-temperature rheological properties of asphalt were tested by temperature sweep mode and multiple stress creep mode of dynamic shear rheometer. The low-temperature rheological properties of asphalt were tested by force ductility meter and bending beam rheometer.

(1) According to the test specification (JTG E20-2011, T 0628), the dynamic shear rheometer was used for temperature sweep mode. The parallel plate size was 25 mm, and the parallel plate spacing was 1 mm; the strain control mode was adopted in the experiment. The strain was controlled at 12%, and the experimental frequency was 10 Hz. The scanning began at 46 °C, and the temperature step was 6 °C. The variation laws of complex modulus (G) and phase angle (δ) of asphalt with temperature were obtained, and the rutting factor (G/sinδ) was calculated to characterize the ability of asphalt to resist high-temperature deformation.

(2) According to the test specification (JTG E20-2011, T 0628), the dynamic shear rheometer was used for multiple stress creep test. The test parameters were set as follows: the diameter of parallel plate was 25 mm, and the spacing of parallel plate was 1 mm. In order to reflect the creep recovery of asphalt under light and heavy traffic loads, the load levels are 0.1 kPa and 3.2 kPa, respectively. The temperature of the test was 64 °C, the load loading time was 1 s, and the unloading time was 9 s, with 10 cycles of repetition. In order to analyze the high-temperature rheological properties of asphalt based on MSCR, the creep recovery rates R@0.1, R@3.2 and unrecoverable creep compliance Jnr@0.1, Jnr@3.2 of asphalt were calculated. The calculation is shown in Eqs. (2) and (3).

$$R = \frac{\gamma_P - \gamma_{nr}}{\gamma_P - \gamma_0} \times 100\% \tag{2}$$

$$J_{nr} = (\gamma_{nr} - \gamma_0)/\tau \tag{3}$$

In Eqs. (2) and (3), γ_0 is the initial strain of each creep recovery period,

γ_P is the peak strain of each creep recovery period,

γ_{nr} is residual strain after recovery stage, and

τ is loading stress, kPa.

(3) According to the test specification (JTG E20-2011, T 0605), the low-temperature force ductility test was carried out by using the force ductility meter. Before the test, the specimen was kept in a water bath at 5 °C for 1.5 h, and the tensile speed was 1 cm/min during the test. The test was stopped until the tensile value was 0. The tensile

flexibility and fracture energy are calculated to characterize the low-temperature performance of asphalt, and the calculation formulas are shown in Eqs. (4) and (5).

$$f = D_{max}/F_{max} \tag{4}$$

$$W = \int_{x=0}^{x=Ductility} F(x)dx \tag{5}$$

In Eq. (4), F_{max} is the maximum tensile force in the tensile process, and

D_{max} is the displacement corresponding to maximum tension.

(4) According to the test procedures (JTG E20-2011, T 0627), the bending creep stiffness test of asphalt was carried out by bending beam rheometer. The creep stiffness (S) and creep rate (m) of asphalt at − 24 °C, − 18 °C, and − 12 °C were tested and calculated by Eqs. (6) and (7). The sample size of the test piece is length 127 mm ± 2.0 mm, height 6.35 mm ± 0.05 mm, and width 12.70 mm ± 0.05 mm. The load during the test is 980 ± 50mN. The low-temperature rheological properties of asphalt mortar were analyzed by indicators such as creep stiffness (S) and creep rate (m) when the beam was bent for 60s.

$$S = (\delta/\varepsilon)_{t=60s;T} \tag{6}$$

$$m = dS(t)/dt|_{t=60s} \tag{7}$$

Characterization of flame retardant mechanism

In order to explore the synergistic enhancement mechanism of nano-clays with different geometry structure on flame retardant performance of asphalt, the thermo-gravimetric/differential scanning calorimeter (TGA/DSC), thermo-gravimetric/Fourier transform infrared spectrometer (TGA/FTIR), and digital camera/scanning electron microscope (DIP/SEM) were used to characterize the material transformation during asphalt combustion.

TGA–DSC was used to test the mass and heat change of asphalt from room temperature to 800 °C under air condition; and effects of TFR, TFR/HNTs, and TFR/OMMT on the decomposition temperature, decomposition rate, heat absorption and desorption, and residue rate of the whole process weight of asphalt combustion were analyzed.

TGA-FTIR was used to test the three-dimensional infrared spectra of the gaseous products formed during the heating process of asphalt from room temperature to 800 °C; and the variation law of the types and yields of gaseous products of asphalt during combustion was analyzed.

DIP-SEM was used to characterize the macro- and micro-morphology of residues formed after combustion of asphalt; the effect of two kinds of nano-clays on the integrity and density of barrier layer was analyzed.

Results and discussion

Flame retardant performance of NFRMA

Static flame retardant performance

The results of static flame retardant performance based on oxygen index instrument and Cleveland opening cup test are shown in Fig. 3. Figure 3a shows that the addition of TFR can significantly improve the flame retardant properties of MA and make it meet the requirements of LOI greater than 23%. The LOI of asphalt shows different changes after compounding two kinds of nano-clays. The LOI of MA/TFR/HNTs first increased and then decreased with the increase of HNTs content, and the optimal content of HNTs was 1.0%. The LOI of MA/TFR/OMMT did not change significantly when the OMMT content was less than 3%, but the LOI showed a decreasing trend when the OMMT content was more than 3%. The LOI increased partially were added alone when 1.0% HNTs and 3.0% OMMTs, but far below the specification requirement, indicating that the nano-clays did not have a significant flame retardant effect when added alone for flame retardant modification of asphalt. Nano-clays increase the viscosity of asphalt, which makes it difficult to melt drops and has a low LOI. Wu et al. [39] proposed the use of SIT to characterize the static combustion properties of asphalt. The higher self-ignition temperature indicates that asphalt is more difficult to burn under the condition of no open flame, and asphalt has better fire safety. It can be seen from Fig. 3b that the SIT of the two kinds of NFRMA gradually increased with the increase of the content of nano-clays,

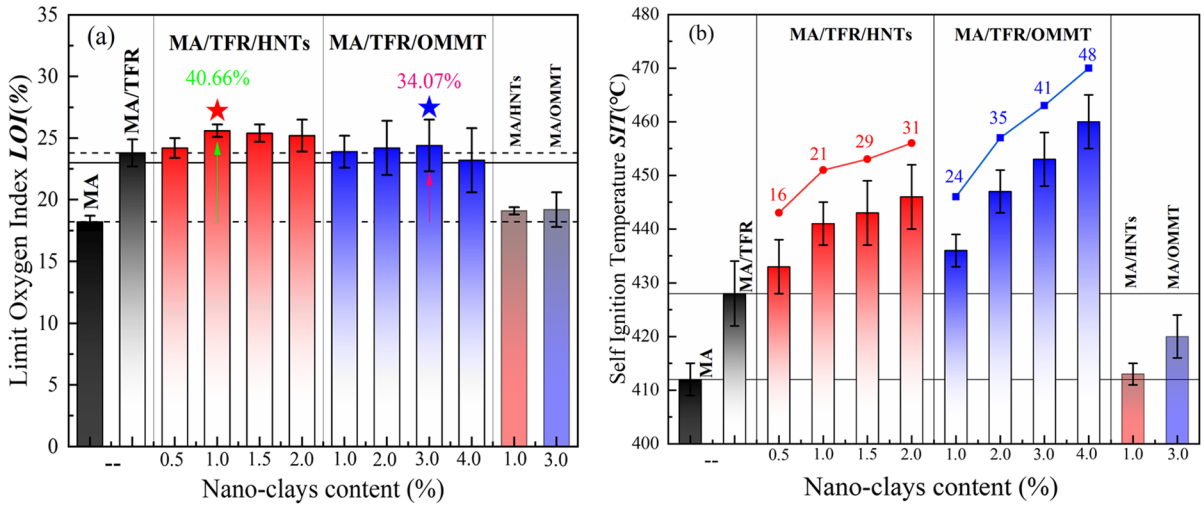

Fig. 3 The static flame retardant performance of NFRMA **a** LOI and **b** SIT

which indicates that HNTs and OMMT are effective in enhancing the difficulty of spontaneous combustion of asphalt under open flame conditions. However, the effect of HNTs and OMMT on the enhancement efficiency of fire safety of flame retardant-modified asphalt could not be compared because of the different dosing amounts of HNTs and OMMT. Li et al. [42] proposed the use of synergistic efficiency (SE) to characterize the effect of composite modifications on the enhancement effect of flame retardant asphalt properties, and the results are shown in Table 5. HNTs and OMMT showed a stronger synergistic efficiency for the increase of LOI and SIT of asphalt. It is noteworthy that lower additions of HNTs have a greater effect on the SIT of MA/FTR, while higher additions of OMMT have a more significant effect on MA/FTR.

Dynamic flame retardant performance

The dynamic flame retardant performance test results of asphalt based on CCT are shown in Fig. 4. Figure 4a and b shows the change of the HRR of asphalt with time under the thermal radiation of 50 kW/m^2. When 8% TFR was added to asphalt, the peak value of HRR of MA/TFR decreased from 993.1 kW/m^2 for MA to 666.6 kW/m^2 (a decrease of 32.88%), which indicates that the addition of TFR can effectively reduce the thermal effect during the combustion of asphalt. When 1.0% HNTs was added into MA/TFR, the peak value of HRR of MA/TFR/1.0%HNTs was about 495.4 kW/m^2. When 3% OMMT was added into MA/TFR, the peak value of HRR of MA/TFR/3%OMMT was about 463.3 kW/m^2. It can be seen that there is no significant difference in the effectiveness of HNTs and OMMT in reducing the heat release rate. This indicates that there is no significant difference in the inhibitory effect of the two kinds of nano-clays on the combustion process of MA/TFR, but the HNTs may have better economy as it can achieve the expected effect with lower dosage. Figure 4c and d is the change of the SPR of asphalt with time under the thermal radiation of 50 kW/m^2. When 8% TFR was added to asphalt,

Table 5 The synergistic efficiency of LOI and SIT of asphalt

	MA/TFR				MA/TFR			
	0.5% HNTs	1.0% HNTs	1.5% HNTs	2.0% HNTs	1.0% OMMT	2.0% OMMT	3.0% OMMT	4.0% OMMT
SE_{LOI}	1.07	1.32	1.29	1.25	1.02	1.07	1.11	0.89
SE_{SIT}	1.31	1.81	1.94	2.13	1.50	2.19	2.56	3.00

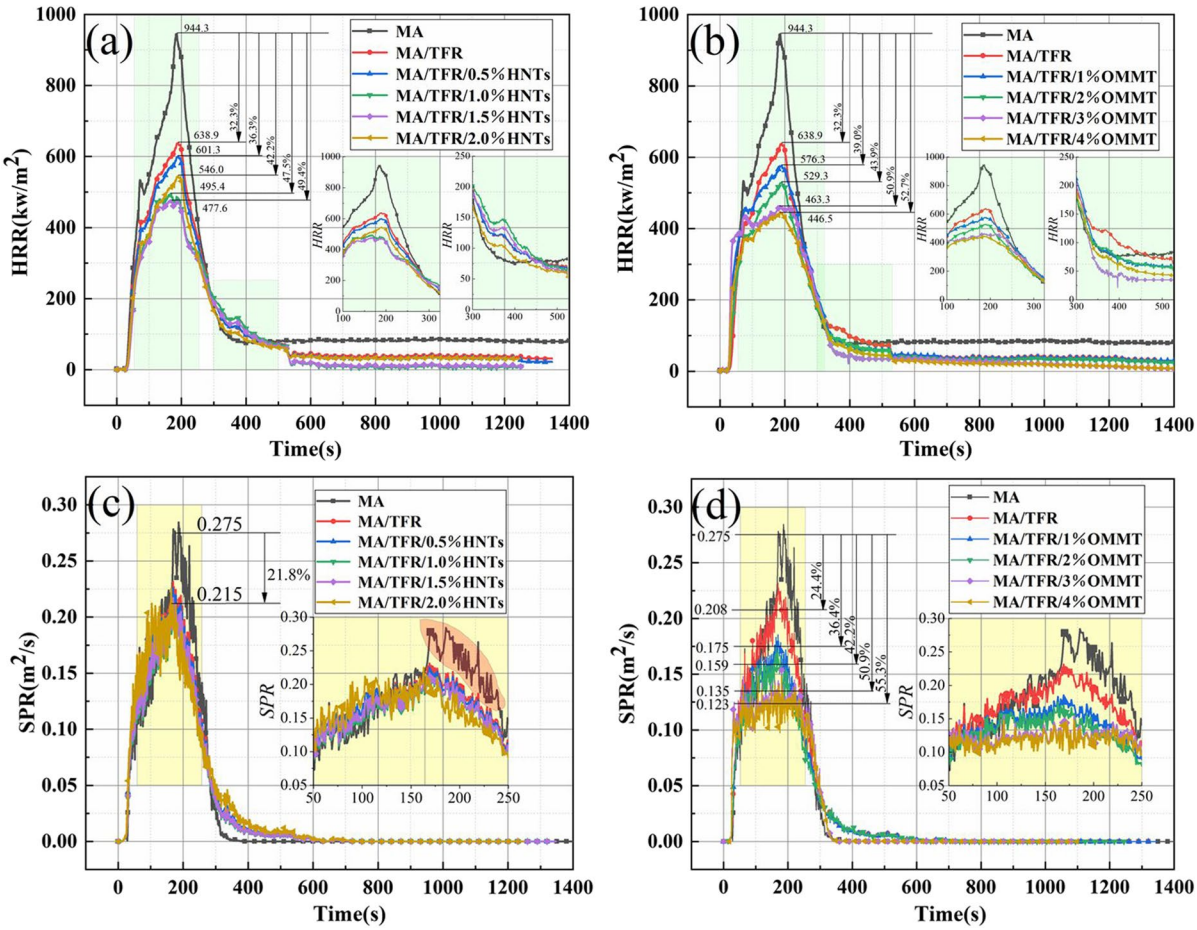

Fig. 4 Dynamic flame retardant properties of NFRMA

the peak value of the smoke release rate of MA can be reduced from 0.279 to 0.231 m^2/s of MA/TFR (a decrease of 17.20%), which indicates that the addition of TFR can inhibit the release of smoke during the combustion of asphalt. When 1.0% HNTs was added into MA/TFR, the peak value of HRR of asphalt did not decrease significantly during the combustion process. When 3.0% OMMT was compounded in MA/TFR, the peak value of SPR of asphalt decreased with the increase of OMMT addition during the combustion process. When the addition of OMMT exceeded 3%, the change of the peak value of SPR of MA/TFR/OMMT was not significant. It indicated that the two kinds of nano-clays had significant differences in the smoke suppression effect of flame retardant asphalt, and MA/TFR/OMMT had more excellent smoke suppression performance.

Rheological properties of NFRMA

High-temperature rheological properties

Temperature sweep test of DSR (DSR-T) The test results of high-temperature rheological properties of asphalt based on DSR-T are shown in Fig. 5. Figure 5a shows the effect of HNTs on the G/sinδ and δ of asphalt in the range of 46 to 82 °C. When 8% TFR was added to MA, the G/sinδ of MA/CFR increased from 4.2 to 6.2 kPa at 64 °C. The upper PG of MA was PG 76, and the upper PG of MA/TFR reached PG 82. At the same time, the addition of TFR reduces the δ of asphalt. It may be due to the absorption of lighter components in the asphalt by the TFR to change the asphalt from a sol–gel state to a gel state with better

high-temperature performance. After adding HNTs to MA/TFR, the G/sinδ was further improved, but the increase was not obvious. When 1.0% HNTs was added to MA/TFR, the G/sinδ of MA/TFR/1.0%HNTs was increased by 27.4% to 7.9 kPa. Figure 5b shows the effect of OMMT on the G/sinδ and δ of asphalt in the range of 46 to 88 °C. The change trend of G/sinδ and δ of MA/TFR/OMMT with temperature is the same as that of MA/TFR/HNTs, but the change degree of each index of MA/TFR/OMMT is higher than that of MA/TFR/HNTs. For example, at 64 °C, the G/sinδ of MA/TFR/3.0%OMMT increased by 70.96% compared with MA/TFR, and the G/sinδ of MA/TFR/1.0% HNTs only increased by 27.4%. The δ of MA/TFR decreased from 81.04 to 72.34° of MA/TFR/3.0%OMMT, while that of MA/TFR/1.0%HNTs was 80.85°; the comparison shows that when the optimal nano-clays content of 1.0% HNTs and 3.0% OMMT is used, the TFR/OMMT flame retardant system improves the high-temperature rheological properties of asphalt more significantly.

Multiple stress creep and recovery test (MSCR) The test results of high-temperature rheological properties of asphalt based on MSCR are shown in Fig. 6. Figure 6a is the creep recovery rate (R) of two kinds of NFRMA at 0.1 kPa and 3.2 kPa, respectively. The creep recovery rate of MA/TFR was both higher than that of MA, indicating that the elastic deformation capacity of MA was enhanced by the addition of TFR into asphalt. With the increase content of nano-clays, the creep recovery rates of MA/TFR/HNTs and MA/TFR/OMMT gradually increased. Among them, the maximum value of the creep recovery rate for MA/TFR/HNTs is still lower than the creep recovery rate for MA/TFR, while the minimum value of the creep recovery rate for MA/TFR/OMMT is higher than the creep recovery rate for MA/TFR. This indicates that the composite of the two kinds of nano-clays has the opposite effect on the MA/TFR elastic deformability. HNTs can reduce the elastic deformation ability of asphalt, and OMMT can improve the elastic deformation ability of asphalt. This may be due to the reinforcing effect of the tubular nano-clays (HNTs) in the asphalt, which makes the asphalt more resistant to deformation. The stresses of 0.1 kPa and 3.2 kPa make the deformation of MA/TFR/HNTs smaller, so the recovery rate of deformation of MA/TFR/HNTs is not obvious. The layered nano-clays (OMMT) does not affect the elastic deformation of asphalt, but the deformation recovery rate of MA/TFR/OMMT is increased due to the high deformation resistance of the layered nano-clays [32, 43]. Figure 6b shows the non-recoverable creep compliance (Jnr) of MA/TFR, MA/TFR/HNTs, and MA/TFR/OMMT at 0.1 kPa and 3.2 kPa, respectively. TFR makes the Jnr@0.1 and Jnr@3.2 of MA/TFR increase compared to that of MA, indicating that the addition of TFR makes MA/TFR less able to resist permanent deformation. The two kinds of nano-clays led to a further reduction of Jnr of asphalt compared to that of MA/TFR, indicating that NCFR can significantly improve the ability of asphalt to resist permanent deformation at 0.1 kPa and 3.2 kPa. The Jnr of MA/TFR/1% HNTs is less than the Jnr of MA/TFR/3%. OMMT is less than the Jnr of MA, which indicates that HNTs improve the resistance

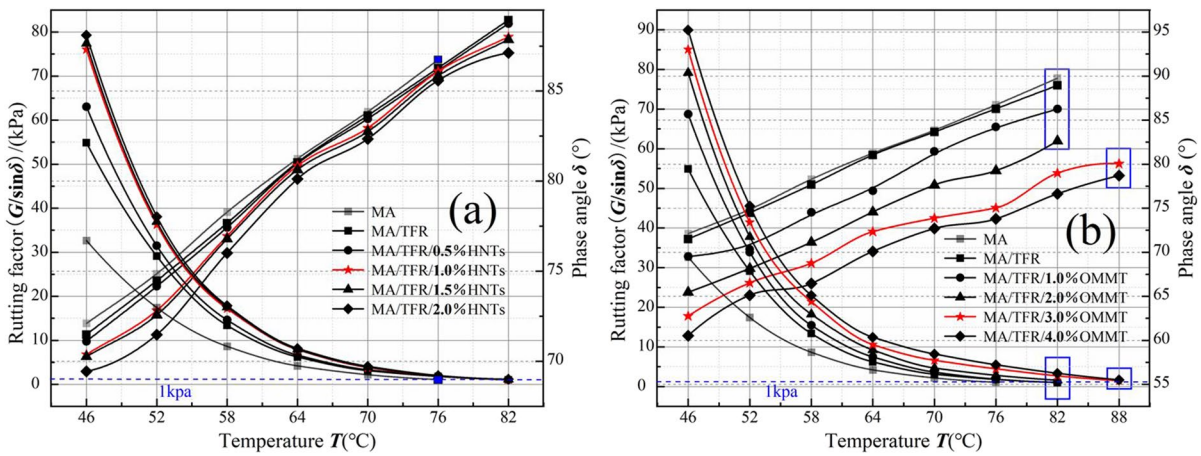

Fig. 5 High-temperature rheological characteristics of NFRMA based on DSR-T

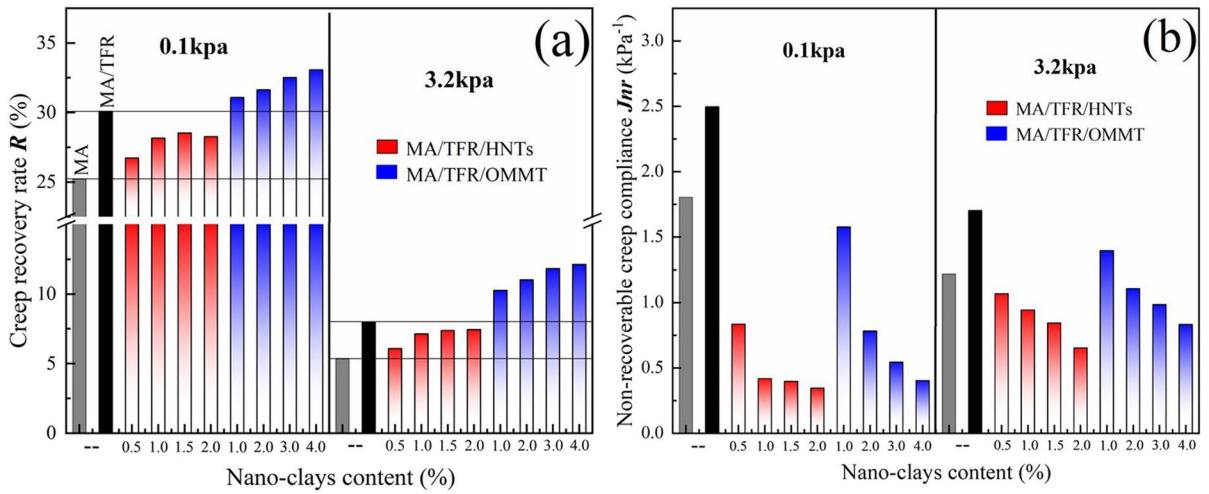

Fig. 6 High-temperature rheological properties of NFRMA based on MSCR

of asphalt to permanent deformation mainly by reducing the amount of deformation each time, while OMMT improves the resistance of asphalt to permanent deformation mainly due to the higher deformation recovery rate, but in general, HNTs are more capable in improving the permanent deformation of asphalt [43, 44].

In summary, TFR, HNTs, and OMMT can effectively improve the high-temperature rheological properties of asphalt based on G, G/sinδ, R, and Jnr. The flame retardant system of TFR/OMMT improves the recovery rate of high-temperature deformation of asphalt more significantly, and the flame retardant system of TFR/HNTs improves asphalt resistance to permanent deformation more significantly. The flame retardant system of TFR/OMMT and TFR/HNTs are both effective in enhancing the resistance of asphalt to high-temperature deformation.

Low-temperature rheological properties

Force ductility test (FDT) The test results of low-temperature rheological properties of asphalt based on FDT are shown in Fig. 7. Figure 7a shows the effect of TFR and two kinds of nano-clays on the tensile flexibility of asphalt. Figure 7b shows the effect of TFR and two kinds of nano-clays on the fracture energy of asphalt. The addition of TFR to MA reduces the flexibility and fracture energy of MA/TFR, which is mainly due to the absorption of lighter components in the asphalt by TFR, which increases the modulus of the asphalt and thus reduces the tensile flexibility of the asphalt under tensile loading and makes the asphalt more prone to brittle fracture. The flexibility and fracture energy of asphalt showed different variations when the two nano-clays were compounded with TFR-modified asphalt separately. With the increase of HNT content, the tensile flexibility and fracture energy of MA/TFR/HNTs first increased and then decreased, and the flexibility of MA/TFR/1%HNTs was 0.087 mm/N increased by 41.5% compared with 0.075 mm/N of MA/TFR but still lower than the flexibility of MA. The fracture energy of MA/TFR/1%HNTs is 312.7N·cm higher than that of MA/TFR. With the increase of OMMT content, the flexibility and fracture energy of MA/TFR/OMMT gradually decrease, the degree of flexibility decrease is not obvious, but the decrease of fracture energy is very significant. Among them, the fracture energy of MA/TFR/3% OMMT (115.4 mm/N) decreases by 47.8% compared to that of MA/TFR (220.9 mm/N). Both flexural and fracture energy indicate that the addition of HNTs makes the low-temperature performance of MA/TFR improve, which may be due to the reinforcing effect of tubular nano-clays, while the addition of OMMT makes the low-temperature performance of asphalt deteriorate, which may be due to the fact that the layers in layered

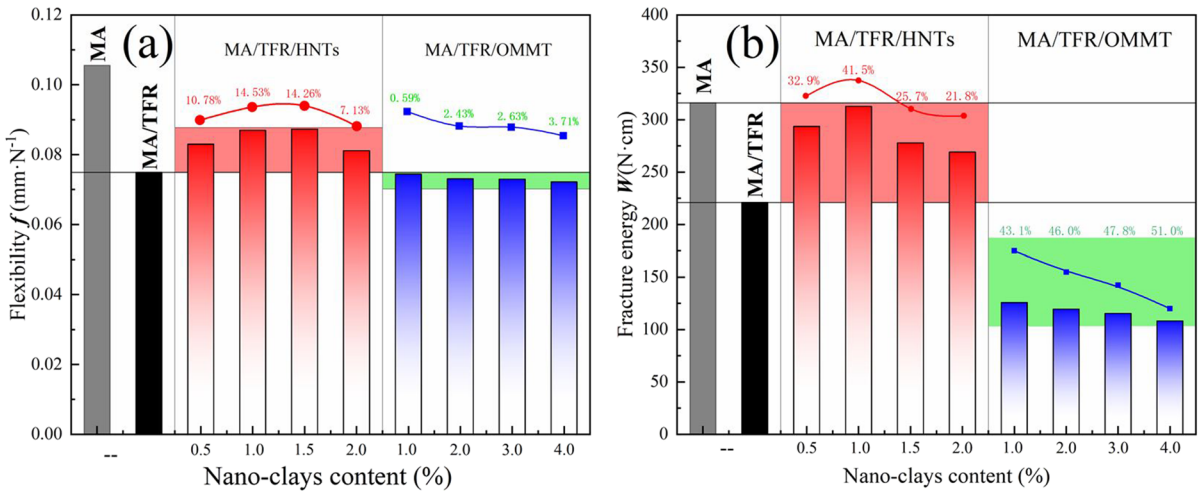

Fig. 7 Low-temperature rheological properties of NFRMA based on FDT

nano-clays are mainly bound by intermolecular forces and are weak interfaces for tensile fracture. However, it is worth noting that whether layered nano-clays deteriorate the low-temperature properties of asphalt depends on the dispersion of the layered nano-clays in the asphalt. When the dispersion is good, the laminated nano-clays uniformly dispersed in the asphalt in a monolayer lamellar structure will have an improved effect on the low temperature of the asphalt.

Bending beam rheometer test (BBR) The test results of low-temperature rheological properties of asphalt based on BRR are shown in Fig. 8. Figure 8a shows the effect of TFR and two kinds of nano-clays on the creep rate of asphalt. The higher creep rate indicates that the asphalt has more deformation per unit time, which means that the asphalt has better ductility at low temperatures. The addition of TFR reduces the low-temperature creep rate of asphalt. When HNTs was compounded in MA/TFR, the creep rate of MA/TFR/HNTs obviously recovered compared to the creep rate of MA/TFR, but did not recover to the level of MA, indicating that HNTs had a function of partially improving the low-temperature performance of MA/TFR, but the improvement effect was limited, and the low-temperature performance of MA/TFR/HNTs was still lower than that of MA. When OMMT was compounded in MA/TFR, the creep rate of MA/TFR/HNTs continued to decrease with the increase of OMMT content, indicating that OMMT would continue to degrade the low-temperature performance of MA/TFR. Figure 8b shows the effects of TFR and two kinds of nano-clays on the creep stiffness of asphalt. The smaller the modulus of creep strength indicates that the asphalt is easier to deform per unit time, and the asphalt's low-temperature deformation ability is stronger. The addition of TFR makes the creep stiffness of asphalt significantly increase. When HNTs were compounded with MA/TFR, the creep stiffness of MA/TFR/HNTs decreased compared with MA/TFR, and the creep stiffness continued to increase with the increase of HNTs, but was not higher than that of MA/TFR. This means that the low-temperature performance of MA/TFR/HNTs is between MA and MA/TFR and HNTs can improve the low-temperature performance of asphalt. When OMMT was compounded in MA/TFR, the creep stiffness of MA/TFR/OMMT increased compared to MA/TFR. The creep stiffness of MA/TFR/OMMT continued to increase as the content of OMMT increased, indicating that OMMT degrades the low-temperature properties of asphalt. It is worth noting that creep rate and creep stiffness showed the same pattern at − 18 °C and − 12 °C, indicating that temperature did not affect the mechanism of action of TFR, HNTs, and OMMT on the low-temperature properties of asphalt [32, 45].

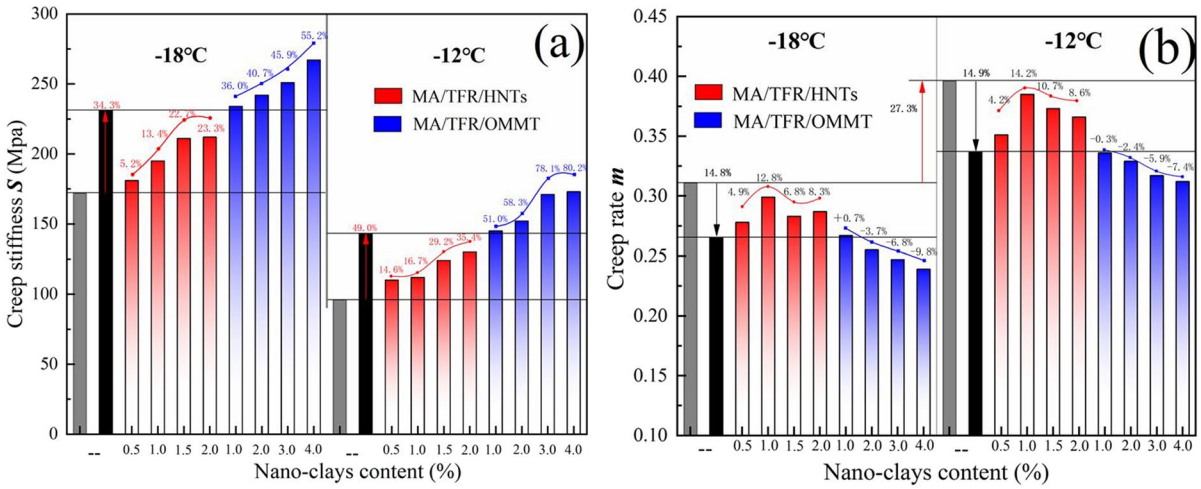

Fig. 8 Low-temperature rheological properties of NFRMA based on BBR

In summary, the low-temperature rheological properties of asphalt are evaluated based on f, W, m, and S. TFR significantly deteriorates the low-temperature performance of asphalt. TFR combined with HNT-modified asphalt can effectively improve the low-temperature performance of asphalt, and TFR combined with OMMT-modified asphalt will further deteriorate the low-temperature performance of asphalt.

Flame retardant mechanism of NFRMA

According to the research on the static and dynamic flame retardant performances and high- and low-temperature rheological properties of the above two kinds of nano-clays composite TFR-modified asphalt, it is found that when the 8% TFR-modified asphalt is respectively adapted to 1%HNTs and 3%OMMT, it has good comprehensive performance. Subsequently, MA/TFR, MA/TFR/1.0%HNTs, and MA/TFR/3.0%OMMT are selected to compare the effects of two kinds of nano-clays with geometric structures on the flame retardant mechanism of MA/TFR.

TGA–DSC

Figure 9a shows the variation of the mass of flame retardant asphalt with temperature. The 5% mass loss temperatures of three kinds of flame retardant-modified asphalt were 347 °C, 367 °C, and 381 °C, which showed that the high-temperature stability of MA/TFR/3.0%OMMT was the best. There was no significant difference in the temperature of asphalts at 50% mass loss, which were 480 °C, 477 °C, and 479 °C, respectively. The final char yield at 800 °C was 13.27% (1st) of MA/TFR/1.0%HNTs, 11.91% (2nd) of MA/TFR/3.0%OMMT, and 9.68% (3rd) of MA/TFR, which indicated that MA/TFR/1.0%HNTs made the highest carbon residue rate of asphalt and could better play the role of barrier layer. Figure 9b shows the mass loss rate of flame retardant-modified asphalt changing with temperature. It was found that the decomposition of MA/TFR and MA/TFR/1.0%HNTs could be divided into four main stages by Gaussian peak fitting method, while MA/TFR/3.0%OMMT was mainly divided into three stages. Compared with each decomposition peak of MA/TFR and MA/TFR/1.0% HNTs, it was found that the rate of the second decomposition stage of MA/TFR was fast, indicating that HNTs had a significant inhibitory effect on the decomposition stage, while the rate of the decomposition stage of MA/TFR/3.0%OMMT was accelerated due to the absence of the first stage. At the same time, the addition of HNTs and OMMT into the asphalt makes the last decomposition stage end at a higher temperature. Figure 9c shows the heat absorption of three kinds of flame retardant-modified asphalt changes

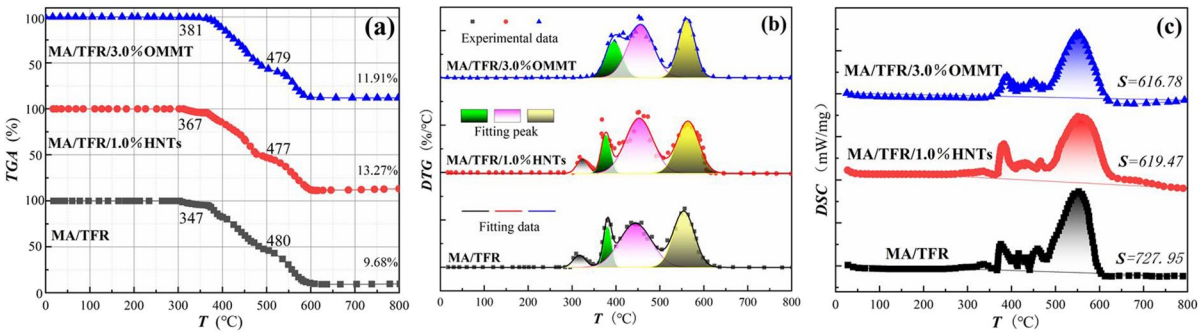

Fig. 9 The changes of weight and heat during asphalt combustion

with temperature. According to the final calculation results, the heat release amounts were 727.95 mW/mg (MA/TFR), 619.47 mW/mg (MA/TFR/1%HNTs), and 616.78 mW/mg (MA/TFR/3%OMMT), respectively. Compared with MA/TFR, the heat release of two kinds of NFRMA (MA/TFR/1%HNTs and MA/TFR/3%OMMT) were reduced by 14.9% and 15.3%, respectively. TGA-DTG-DSC data show that the effect of heat absorption through decomposition of both NFRMAs on asphalt combustion is not significant, mainly due to the increase in thermal stability of asphalt by NFR and thus the shift of asphalt combustion to higher temperatures. Shi et al. [46] showed that the shift of asphalt combustion to the higher temperature range increases the agglomeration of heavy components and thus increases the residue generation rate, which also explains the increase in the amount of NFRMA residue.

TGA-FTIR

The 3D-FTIR of the gaseous products of flame retardant-modified asphalt changes with temperature is shown in Fig. 10. The results show that there is no obvious change in the characteristic peaks of 3D-FTIR of flame retardant asphalt, which shows that there is no significant difference in the types of gaseous products of the three kinds of flame retardant-modified asphalt, but the content of various gaseous products at different temperatures is significantly different. Before 300 °C, there was no obvious characteristic peak of asphalt, indicating that asphalt had good thermal stability and no obvious flue gas generation. With the increase of temperature, the gaseous products of three kinds of flame retardant-modified asphalt are mainly divided into two stages: 300 to 500 °C and 500 to 650 °C. The characteristic peaks of gaseous products are concentrated in 2400–2200 cm^{-1} and 700–500 cm^{-1}, which coincides with the main temperature range of asphalt decomposition, indicating that asphalt decomposition will release a large number of gaseous products. At the same time, there are obvious differences in the peak intensity of the 3D-FTIR of the three kinds of asphalt, and the order of the three is MA/TFR/3.0%OMMT, MA/TFR/1.0%HNTs, and MA/TFR, which shows that OMMT has high efficiency in inhibiting the formation of phase products during the thermal decomposition of asphalt [29].

DIP-SEM

The macro-morphology and micro-morphology of residues formed after combustion of three kinds of flame retardant-modified asphalt are shown in Fig. 11. Figure 11 (a) and (a_1) show the macro-morphology and micro-morphology of the residue after MA/TFR combustion, indicating that TFR can make asphalt form a relatively complete barrier layer structure, but the strength of the barrier layer is low, the surface layer is easily broken, and the integrity is not good. Figure 11 (b) and (b_1) show the macro-morphology and micro-morphology of the residue after MA/TFR/1.0%HNTs combustion, indicating that the compound HNTs can significantly enhance the thickness and integrity of the residue, so as to effectively play the role of barrier layer. Figure 11 (c) and (c_1) show the macro-morphology and micro-morphology of the residue after MA/TFR/3.0%OMMT combustion,

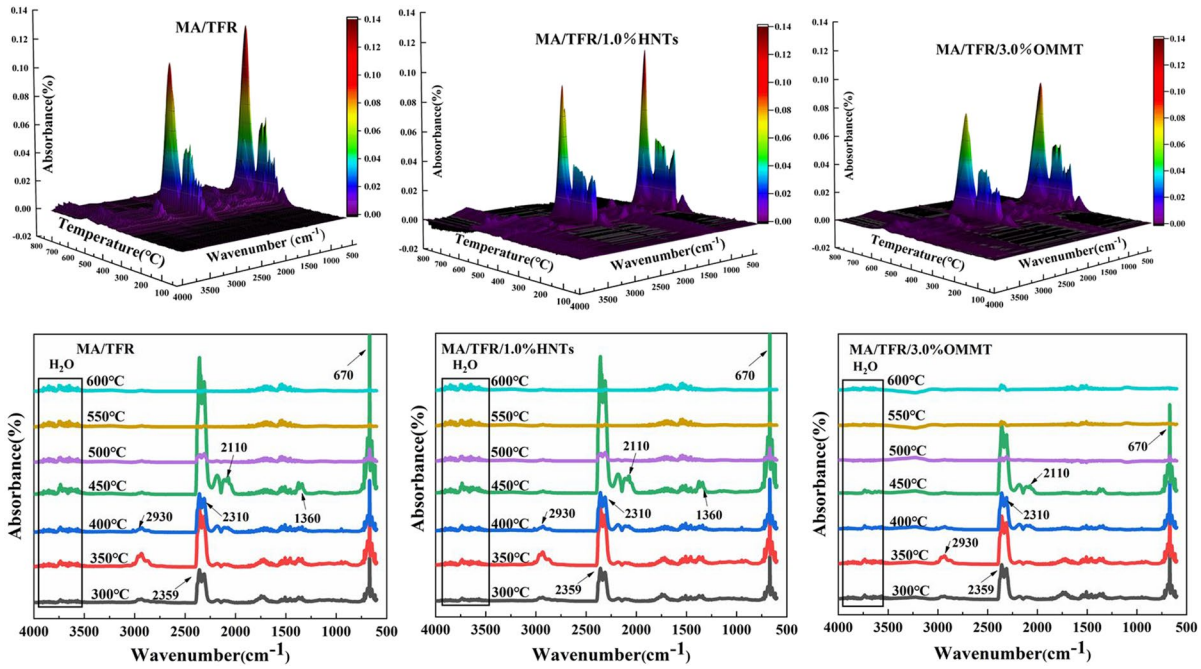

Fig. 10 FTIR of gaseous products during asphalt combustion

indicating that the composite OMMT can effectively increase the hardness and compactness of the barrier layer. However, it may be due to the large lamellar structure of OMMT that it fails to form a smooth structure when forming the barrier layer, and there are obvious cracks. The flame retardant mechanism of nano-clays was summarized and shown in Fig. 12.

In order to better compare the effect mechanisms of nano-clays on flame retardant-modified asphalt, the flame retardant mechanism of nano-clays is summarized and shown in Fig. 12. The combustion of asphalt is divided into three main stages: stage 1, heat-absorbing flame retardant; stage 2, catalytic flame retardant; and stage 3, barrier layer effect. Stage 1: ATH in the three kinds of flame retardant-modified asphalt competes with asphalt to absorb heat, improve the thermal stability of asphalt, and reduce the organic volatiles in stage 1. It is worth noting that the yield of organic volatiles in this stage will largely affect the burning process of asphalt, and if the yield of organic volatiles is high, it will make asphalt burn early [47]. Nano-clays do not have the same mechanism to inhibit the production of organic volatiles in asphalt at stage 1. MA/TFR/1.0%HNTs inhibit the flow of molecules inside the asphalt mainly through the reinforcing effect of the tubular structure of HNTs, which manifests itself as an increase in the viscosity of the asphalt [34]. MA/TFR/3%OMMT not only has the above effect but also increases the length of the channels for small molecule precipitation due to the barrier effect of the layered structure, which makes it more difficult for the gas to precipitate [22, 34]. Stage 2: The ADP in the three kinds of flame retardant-modified asphalt can decompose to produce phosphorus radicals. A part of the radicals into the flame zone, its ability to neutralize the high-energy radicals interrupt the process of combustion reaction in the flame. Another part of the phosphorus radicals remain in the asphalt, its ability to promote the conversion of organic molecules in asphalt to heavy components, which facilitates the formation of surface carbon layer [32]. The flame retardant mechanism of nano-clays at this stage is that the disintegration of tubular and lamellar structures will produce lewis acidic sites capable of catalyzing the carbon formation of asphalt [$^{+}$48]. Nano-clays are a thermally stable silicate material, and the small molecules produced by the decomposition of the asphalt will drive the nano-clays to migrate to the surface, thus acting as a surface barrier layer over the asphalt surface. Stage

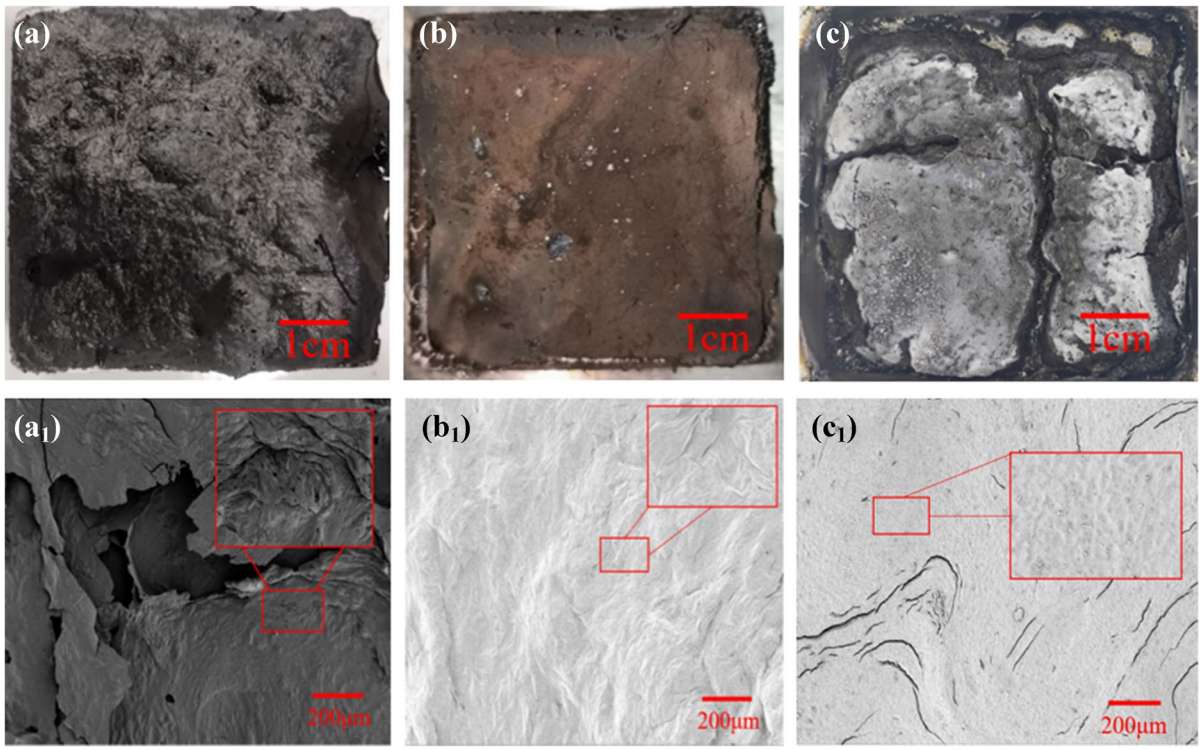

Fig. 11 Macro-morphology and micro-morphology of residue

3: The flame retardant makes the asphalt form different barrier layers on the surface, and the state of the barrier layer determines whether the asphalt will continue to burn or not. MA/TFR cannot achieve good flame retardant effect due to low carbon formation efficiency and incomplete carbon layer structure. The barrier layer on the surface of MA/TFR/1% HNTs is homogeneous and stable, which has a good barrier to heat mass exchange and makes asphalt burning stop. The structure of the barrier layer on the surface of MA/TFR/3%OMMT is not complete, but still has a certain flame retardant effect.

Conclusions

(1) Nano-clays composite 8% TFR-modified asphalt has obvious synergistic effect; the optimum contents of HNTs and OMMT are 1.0% and 3.0%, respectively. The flame retardant performance of MA/TFR/1.0%HNTs was significantly improved compared with that of MA/TFR/3.0%OMMT, while MA/TFR/3.0%OMMT had more obvious smoke suppression performance.

(2) Nano-clays can effectively improve the high-temperature performance of asphalt, especially MA/TFR/3.0% OMMT. The effect of two kinds of nano-clays on the low-temperature performance of asphalt is obviously different. The low-temperature performance of MA/TFR/1%HNTs is improved compared with MA/TFR, indicating that HNTs can repair the deterioration of low-temperature performance of asphalt by TFR. While the low-temperature performance of MA/TFR/3.0%OMMT is worse than that of MA/TFR, the incorporation of OMMT will continue to deteriorate asphalt low-temperature crack resistance.

(3) The flame retardant mechanism of two kinds of nano-clays composite TFR-modified asphalt is similar, mainly reflected in three aspects: endothermic flame retardant, catalytic flame retardant, and barrier layer effect. However, there are still some differences: ① From the aspect of thermogravimetric change, OMMT has obvious inhibi-

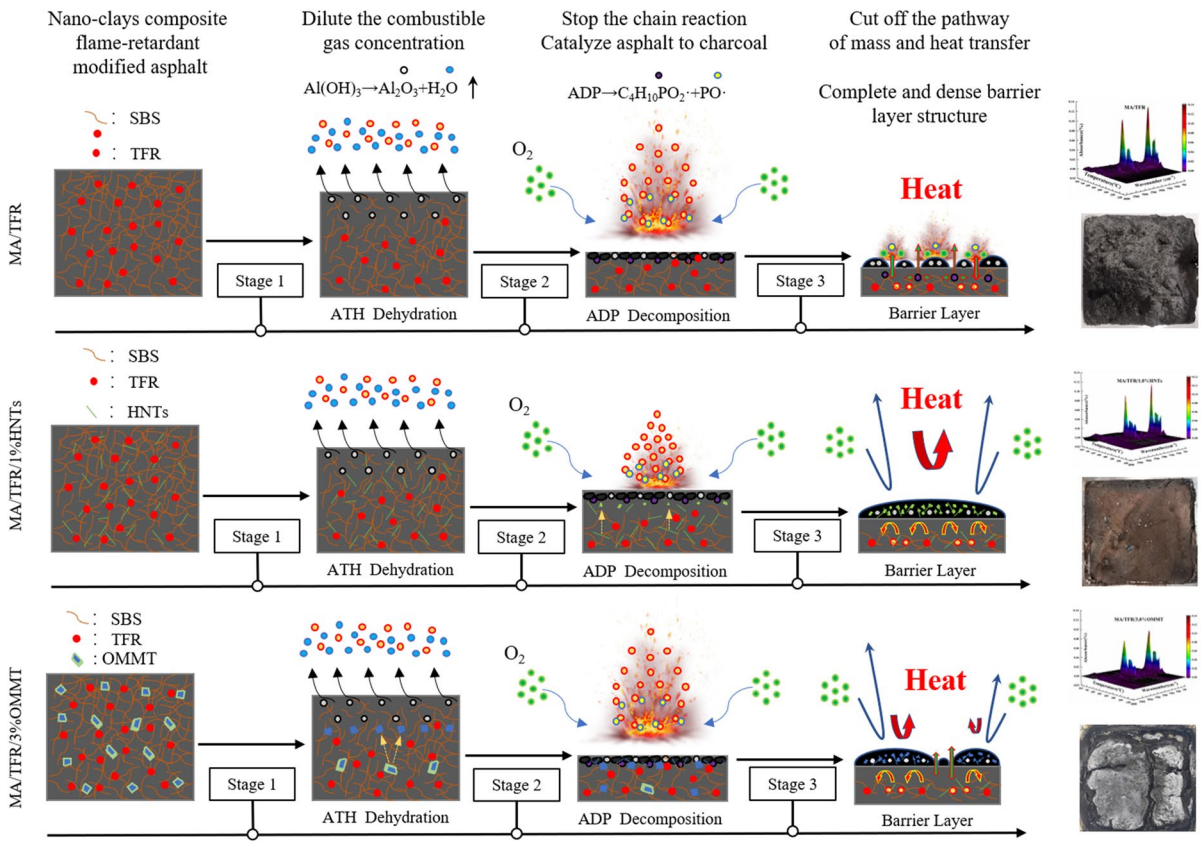

Fig. 12 Flame retardant mechanism of NFRMA

tory effect on the decomposition of asphalt in the early stage, while MA/TFR/1.0%HNTs has a larger carbon residue rate with a smaller content, which is more conducive to the formation of surface barrier layer. ② From the comparison of gaseous products: MA/TFR/3%OMMT significantly inhibited the formation of gaseous products compared to MA/TFR/1%HNTs. ③ Comparison of the macro- and micro-morphology of the residue: OMMT and HNTs can effectively increase the thickness and stability of barrier layer, but the barrier layer of MA/TFR/3%OMMT has obvious cracks, and MA/TFR/1%HNTs make the barrier layer structure more uniform and stable.

Acknowledgements All the authors of the following references are much appreciated.

Author contribution Yangwei Tan: Investigation, conceptualization, writing—original draft, writing—review. Jianguang Xie: Writing—review, supervision, project administration. Zhanqi Wang: Data curation and analysis. Kuan Li: Writing—review, conceptualization. Zhaoyi He: Methodology, writing—review

Funding This research was supported by the National Natural Science Foundation of China (51978116) and Graduate Scientific Research and Innovation Foundation of Chongqing, China (Grant No. CYS20283).

Data availability Data will be made available on request.

Declarations

Conflict of interest The authors declare no competing interests.

References

1. Qiu JL, Yang T, Wang XL, Wang LX, Zhang G (2019) Review of the flame retardancy on highway tunnel asphalt

pavement. Constr Build Mater 195:468–482. https://doi.org/10.1016/j.conbuildmat.2018.11.034
2. Chen R, Zhao RK, Liu Y, Xi ZH, Cai J, Zhang JS, Wang QJ, Xie HF (2021) Development of eco-friendly fire-retarded warm-mix epoxy asphalt binders using reactive polymeric flame retardants for road tunnel pavements. Constr Build Mater 284:122752. https://doi.org/10.1016/j.conbuildmat.2021.122752
3. Xu T, Huang XM (2010) Study on combustion mechanism of asphalt binder by using TG-FTIR technique. Fuel 89:2185–2190. https://doi.org/10.1016/j.fuel.2010.01.012
4. Xia WJ, Wang SW, Wang H, Xu T (2021) Inhibitory effects of developed composite flame retardant on bituminous combustion and volatile emissions. J Clean Prod 279:123538. https://doi.org/10.1016/j.jclepro.2020.123538
5. Xiao FP, Guo R, Wang JG (2019) Flame retardant and its influence on the performance of asphalt - a review. Constr Build Mater 21:841–861. https://doi.org/10.1016/j.conbuildmat.2017.01.064
6. Ding QJ, Liu XQ, Shen F, Hu SG (2008) Test and mechanism analysis of ATH asphalt flame-retarding system. China J Highw Transp 21(5):10–14. https://doi.org/10.19721/j.cnki.1001-7372.2008.05.003
7. Huang ZY, Wu B, Kang C, Zhu KWuK (2016) Flame retardant and pavement performance of composite hydroxide modified asphalt. J Zhejiang Univ 50(1):27–32. https://doi.org/10.3785/j.issn.1008-973X.2016.01.05
8. Yang XL, Wang GC, Liang MM, Yuan TP, Rong HL (2021) Effect of aluminum hydroxide (ATH) on flame retardancy and smoke suppression properties of SBS-modified asphalt. Road Mater Pavement 2021:2012239. https://doi.org/10.1080/14680629.2021.2012239
9. Ling TQ, Zhang RZ, Ning HY, Yuan M (2011) Study on flame retardant performance of intumescent asphalt flame retardant. J Chongqing Jiaotong Univ 30(5):948–951+988. https://doi.org/10.3969/j.issn.1674-0696.2011.05.014
10. Jin L, Wei JG, Fu QL, Zhang QJ (2020) Effect of DBDPE composite flame retardant on the performance of SBS asphalt. J Chang'an Univ 40(02):47–55+65. https://doi.org/10.19721/j.cnki.1671-8879.2020.02.006
11. He LP, Shen AQ, Liang JL, Xie C (2013) Flame retardant and pavement performance of flame retardant asphalt and asphalt mixture. J Highw Transp Res Dev 30(12):15–22. https://doi.org/10.3969/j.issn.1002-0268.2013.12.003
12. Wei JG, Xie C, Fu QL (2013) Influence of flame retardant on technical performances of asphalt and asphalt Mixture. China J Highw Transp 26(6):30–37. https://doi.org/10.19721/j.cnki.1001-7372.2013.06.005
13. Qin XT, Zhu SY, Chen SF, Deng KY (2013) The mechanism of flame and smoke retardancy of asphalt mortar containing composite flame retardant material. Constr Build Mater 41:852–856. https://doi.org/10.1016/j.conbuildmat.2012.12.048
14. Tan YQ, Lan BW, Ji L, Shang YF (2009) Modified techniques of commonly-used flame-retardant asphalt in asphalt pavement tunnel. J Chongqing Jiaotong Univ 28(4):711–719. 1674–0696(2009)04–0711–04
15. Fu QL, Wei JG, Peng WJ, Jin L (2020) Performance and flame retardant mechanism of coordinated flame retardant asphalt with DBDPE and Sb_2O_3. China J Highw Transp 33(02):44–55. https://doi.org/10.19721/j.cnki.1001-7372.2020.02.004
16. Yang XL, Shen AQ, Guo YC, Wu HS, Wang H (2021) A review of nano layered silicate technologies applied to asphalt materials. Road Mater Pavement 22(8):1708–1733. https://doi.org/10.1080/14680629.2020.1713199
17. Li RY, Xiao FP, Amirkhanian S, You ZP, Huang J (2017) Developments of nano materials and technologies on asphalt materials – a review. Constr Build Mater 143(15):633–648. https://doi.org/10.1016/j.conbuildmat.2017.03.158
18. Daniel GG, David GS, Vicent F, Juan LM, Rafael B (2018) Improvement of mechanical and thermal properties of poly(3-hydroxybutyrate) (PHB) blends with surface-modified halloysite nanotubes (HNT). Appl Clay Sci 162:487–498. https://doi.org/10.1016/j.clay.2018.06.042
19. Olawale MS, Abdelkibir B, Nourredine AH (2020) Clays and carbon nanotubes as hybrid nanofillers in thermoplastic-based nanocomposites – a review. Appl Clay Sci 185:105408. https://doi.org/10.1016/j.clay.2019.105408
20. Eleni GK, Eleni GI, Konstantinos A, Dimitrios P (2021) Applications of halloysite in tissue engineering. Appl Clay Sci 214:106291. https://doi.org/10.1016/j.clay.2021.106291
21. Yang XL, Shen AQ, Jiang YX, Meng YJ, Wu HS (2021) Properties and mechanism of flame retardance and smoke suppression in asphalt binder containing organic montmorillonite. Constr Build Mater 302:124148. https://doi.org/10.1016/j.conbuildmat.2021.124148
22. Zhang HL, Shi CJ, Han J, Yu JY (2013) Effect of organic layered silicates on flame retardancy and aging properties of bitumen. Constr Build Mater 40:1151–1155. https://doi.org/10.1016/j.conbuildmat.2012.11.097
23. Zhu K, Tang DQ, Huang YD, Wang Q, Wu K (2019) Mechanism of flame and smoke retardancy of asphalt with ZnMgAl-CO_3-LDHs. J Build Mater 22(04):599–605. https://doi.org/10.3969/j.issn.1007-9629.2019.04.014
24. Zhu K, Wang YH, Tang DQ, Wang Q, Li HH, Huang YD, Huang ZY, Wu K (2019) Flame-retardant mechanism of layered double hydroxides in asphalt binder. Materials 12:801. https://doi.org/10.3390/ma12050801
25. Shen AQ, Wu HS, Guo YC, Yang XL, He ZM, Li Y (2021) Effect of layered double hydroxide on rheological and flame-retardant properties of styrene-butadiene-styrene modified asphalt. J Mater Civ Eng 33(2):04020454. https://doi.org/10.1061/(ASCE)MT.1943-5533.0003534
26. Li ML, Pang L, Chen MZ, Xie J, Liu QT (2018) Effects of aluminum hydroxide and layered double hydroxide on asphalt fire resistance. Materials 11:11101939. https://doi.org/10.3390/ma1110193
27. Bonati A, Merusi F, Bochicchio G, Tessadri B, Polacco G, Filippi S, Giuliani F (2013) Effect of nanoclay and conventional flame retardants on asphalt mixtures fire reaction. Constr Build Mater 47:990–1000. https://doi.org/10.1016/j.conbuildmat.2013.06.002
28. Liang YS, Yu JY, Feng ZG, Ai PS (2013) Flammability and thermal properties of bitumen with aluminium trihydroxide and expanded vermiculite. Constr Build Mater

48:1114–1119. https://doi.org/10.1016/j.conbuildmat.2013.07.074
29. Yang XL, Shen AQ, Su YX, Zhao WD (2020) Effects of alumina trihydrate (ATH) and organic montmorillonite (OMMT) on asphalt fume emission and flame retardancy properties of SBS-modified asphalt. Constr Build Mater 236:117576. https://doi.org/10.1016/j.conbuildmat.2019.117576
30. Tan YW, He ZY, Li X, Jiang B, Li JQ, Zhang YG (2020) Research on the flame retardancy properties and mechanism of modified asphalt with halloysite nanotubes and conventional flame retardant. Materials 13(20):4509. https://doi.org/10.3390/ma13204509
31. Li JQ, He ZY, Yu L, He L, Shen ZZ (2021) Multi-objective optimization and performance characterization of asphalt modified by nanocomposite flame-retardant based on response surface methodology. Materials 14:4367. https://doi.org/10.3390/ma14164367
32. Tan YW, Xie JG, Wu YF, Wang ZQ, He ZY (2023) Performance and microstructure characterizations of halloysite nanotubes composite flame retardant modified asphalt. J Mater Civ Eng 35(3):04022448. https://doi.org/10.1061/(ASCE)MT.1943-5533.0004630
33. Batistella MA, Sonnier R, Otazaghine B, Petter CO, Lopez-Cuesta JM (2018) Interactions between kaolinite and phosphinate-based flame retardant in Polyamide 6. Appl Clay Sci 157:248–256. https://doi.org/10.1016/j.clay.2018.02.021
34. Pei JZ, Wen Y, Li YW, Shi X, Zhang JP, Li R, Du QL (2014) Flame-retarding effects and combustion properties of asphalt binder blended with organo montmorillonite and alumina trihydrate. Constr Build Mater 72:41–47. https://doi.org/10.1016/j.conbuildmat.2014.09.013
35. Yuan P, Tan DY, Faïza AB (2015) Properties and applications of halloysite nanotubes: recent research advances and future prospects. Appl Clay Sci 112–113:75–93. https://doi.org/10.1016/j.clay.2015.05.001
36. Barick AK, Tripathy DK (2011) Effect of organically modified layered silicate nanoclay on the dynamic viscoelastic properties of thermoplastic polyurethane nanocomposites. Appl Clay Sci 52:312–321. https://doi.org/10.1016/j.clay.2011.03.010
37. Mahsa N, Azam JA, Karim G (2014) Organoclay maleated natural rubber nanocomposite. Prediction of abrasion and mechanical properties by artificial neural network and adaptive neuro-fuzzy inference. Appl Clay Sci 97–98:187–199. https://doi.org/10.1016/j.clay.2014.05.027
38. Vargas MA, Moreno L, Montiel R, Manero O, Vázquezc H (2017) Effects of montmorillonite (Mt) and two different organo-Mt additives on the performance of asphalt. Appl Clay Sci 112–139:20–27. https://doi.org/10.1016/j.clay.2017.01.009
39. Wu K, Huang ZY, Xu X (2009) Research on thermal effect of asphalt pavement combustion in long tunnel fires. China J Highw Transp 22(2):77–81. https://doi.org/10.19721/j.cnki.1001-7372.2009.02.014
40. Bonati A, Rainieri S, Bochicchio G, Tessadri B, Giuliani F (2015) Characterization of thermal properties and combustion behavior of asphalt mixtures in the cone calorimeter. Fire Saf J 74:25–31. https://doi.org/10.1016/j.firesaf.2015.04.003
41. Qian GP, Yu HN, Gong XB, Zheng WF (2019) Effect of phosphorus slag powder on flammability properties of asphalt. J Mater Civ Eng 31(11):1104019280. https://doi.org/10.1061/(ASCE)MT.1943-5533.0002951
42. Li LH, Zou SL, Chen CY (2012) Study on the flame retardant and smoke suppression performance and road performance of flame retardant asphalt mixture. J Build Mater 15(05):648–653. https://doi.org/10.3969/j.issn.1007-9629.2012.05.013
43. Di HB, Zhang H, Yang EH, Ding HB (2023) Usage of Nano-TiO2 or Nano-ZnO in asphalt to resist aging by NMR spectroscopy and rheology technology. J Mater Civ Eng 35(1):04022391. https://doi.org/10.1061/(ASCE)MT.1943-5533.0004570
44. Liu JW, Hao PW, Sun BW, Li Y, Wang YD (2022) Rheological properties and mechanism of asphalt modified with polypropylene and graphene and carbon black composites. J Mater Civ Eng 34(12):04022343. https://doi.org/10.1061/(ASCE)MT.1943-5533.0004513
45. Jia M, Zhang Z, Wei L, Li J, Yuan D, Wu X, Mao Z (2019) High- and low temperature properties of layered silicate-modified bitumens: view from the nature of pristine layered silicate. Appl Sci 9:3563. https://doi.org/10.3390/app9173563
46. Shi HQ, Xu T, Zhou P, Jiang RL (2017) Combustion properties of saturates, aromatics, resins, and asphaltenes in asphalt binder. Constr Build Mater 136:515–523. https://doi.org/10.1016/j.conbuildmat.2017.01.064
47. Tao Xu, Wang Y, Xia WJ, Hu ZH (2018) Effects of flame retardants on thermal decomposition of SARA fractions separated from asphalt binder. Constr Build Mater 173:209–219. https://doi.org/10.1016/j.conbuildmat.2018.04.052
48. Li JS, Wu W, Hu H, Rui ZG, Zhao TY, Zhang XY (2022) The synergism effect of montmorillonite on the intumescent flame retardant thermoplastic polyurethane composites prepared by selective laser sintering. Polym Compos 43(9):5863–5876. https://doi.org/10.1002/PC.26621